



Application thermal research of forced-air cooling system in high-power NPC three-level inverter based on power module block



Shi-Zhou Xu*, Yu-Feng Peng, Shao-Yu Li

College of Electronic and Electrical Engineering, Henan Normal University, Xinxiang, China

ARTICLE INFO

Keywords:

Three-level inverter
NPC
Cooling system
Thermal analysis
Power module block

ABSTRACT

During the process of cooling system design, the traditional method is calculating power losses of power devices, building thermal model of power devices, establishing system structure model, and making thermal analysis. While, the ideal assumptions and complex equivalent models in traditional methods bring in large error and the analysis of whole system model reduces the effectiveness of cooling system design for complicated high-power inverters. In this paper, the power losses of power devices in NPC (*Neutral-Point-Clamped*) three-level inverter based on SVPWM (Space Vector Pulse Width Modulation) was calculated firstly; the input power and cooling power of each power module block were analyzed, and the cooling power of each block supplied by cooling fan was obtained to figure out the cooling fan parameters. The designed forced-air cooling system was proved by finite element simulation. Finally, the temperature rise experiment was carried out on a 1 MW NPC three-level inverter, and the results proved the effectiveness and feasibility of the proposed method.

1. Introduction

The thermal phenomenon in inverters is mainly caused by power losses of power devices. While power devices themselves are sensitive to temperature, and their conducting and switching characteristics will change with it, which will finally affect the performance of inverters. Therefore, accurate power loss calculation can optimize the cooling system design to ensure stable and reliable operation of inverters. At present, there are many researches on single IGBT (Insulated Gate Bipolar Transistor) module and power loss calculation of two-level inverters, and all the methods are similar. However, the NPC three-level inverter is much more complicated comparing with two-level inverters and the power loss calculation of their power devices is different as well. The main reasons are as follow:

- (1) The conducting frequencies of all power devices in each bridge arm are asymmetric;
- (2) Each bridge arm installs additional clamping diodes;
- (3) There are always two power devices working at the same time in any direction of each bridge arm.

In view of different characteristics above, several researches on power loss calculation of NPC three-level inverter were made, while some difference and problems still exist. In [1,2], it is the junction temperature which was ignored during the power loss calculation that caused certain errors between calculation and experiment results. The power losses of power devices in high-power NPC three-level inverter were calculated based on SVPWM modulation in [3], which are the average values in one modulation voltage cycle and are much more accurate. An ideal assumption that switching power loss has a linear relation to withstanding voltage were made both in [4,5]. However, it is valid approximately only within $\pm 20\%$ range of test voltage. In [6], the thermal component model of IGBT was established

* Corresponding author.

E-mail address: xushizhou@sie@163.com (S.-Z. Xu).

<http://dx.doi.org/10.1016/j.csite.2016.10.002>

Received 3 August 2016; Received in revised form 26 September 2016; Accepted 8 October 2016

Available online 15 October 2016

2214-157X/ © 2016 Published by Elsevier Ltd. This is an open access article under the CC BY-NC-ND license (<http://creativecommons.org/licenses/by/4.0/>).

to analyze the electrothermal analysis of IGBT module system. While, it is necessary to build a complicated RC component model to extract thermal resistance and time constants for a thermal network. A practical method was proposed in [7] to design converter cooling system based on power loss calculation of IGBT module, but its design process is complex and lack of experiments in high-power converters. It is considered in [8] that the reverse recovery losses of four anti-parallel diodes in one bridge arm are totally the same, while in fact, the inner two diodes do not withstand voltage and have no reverse recovery losses. In literature [9], a fast power-loss and temperature simulation method was proposed, and the variation of temperature was described as a function of time using Fourier-based solution through the whole inverter power module structure. The power loss of IGBT module was calculated in [10] to design the cooling system with ANSYS, which is useful but has not been used in high-power applications.

Similarly, several researches on forced-air cooling system were made so far. It is expressed in [11,12] that empirical formula and analysis model has been an alternative method to describe a number of different models accurately, and the theory power limit of forced-air cooling system was studied to optimize the heatsink. A fin type array of forced convection cooling plate was described in [13]. A guidance for selecting heatsink and recommendation on design process were offered in [14]. In [15], a comprehensive analysis process was presented and deduced a simple empirical equation, which has enough precision in analysis and design. The electro-thermal analysis of three phase inverter with cooling system was made by simulation in [16], but it is on the basis of equivalent RC thermal model to estimate chip temperature by simulating on water cooling system. In [17], the estimation of power loss considering the junction temperature is introduced and then used the finite element analysis to estimate the peak junction temperature prediction based on the measurement of IGBTs dynamic characteristics. 3-level IGBT modules with trench gate IGBT and their thermal analyses were made in [18], while it is effective only in some special operation modes, such as UPS(Uninterruptible Power Supply), PFC(Power Factor Correction) and PV(Photovoltaic) system.

The purpose of this paper is to propose a simple and effective method to provide theory reference during cooling system design. The principle and modeling of power module block was organized in Section II to illustrate the structure and calculate the power losses of power devices. The total power losses of all power devices in one power module was considered as one power source, which will also act as heat sources in the heatsink of forced-air cooling system model to improve the accuracy of power-loss calculation. In Section III, the model based on the real structure was built and the cooling capacity was analyzed to fix calculate the operation point of cooling fan for selecting suitable fan, which will offer much practical references for inverter system design and improvement. The simulation and experiment were arranged in Section IV to prove the proposed method and a conclusion was drawn in Section V.

2. Principle and modeling of power module block

It can be seen from Fig. 1(a) that phase A,B, and C are composed of IGBT T_1, T_2, T_3, T_4 , freewheeling diode D_1, D_2, D_3, D_4 , and clamping diode D_5, D_6 . The power devices are Infineon FF1400R17IE4 series, which has anti-parallel diode in itself. The distributions of heatsink in inverter and power devices on heatsink are shown in Fig. 1(b).

Due to the symmetry of bridge arm up and down, it is enough to research one bridge arm to measure the cooling performance of the system. The upper bridge arm of phase A is selected in this paper. It is shown in Fig. 2 that $D_5, T_1, D_1, T_2, D_2, T_3$ and D_3 were placed on this heat-sink block surface, where T_3 , and D_3 belong to the lower bridge arm.

In order to avoid complicated mathematical models in [19], a power module block was proposed in this paper. The heatsink shown in Fig. 2 including power devices can be considered as one heat-sink module block. During the process of building thermal model, it only needs calculating power losses of power devices acting as input power. Meanwhile, in accordance with the characteristic parameters of power module block, the operation point and power of cooling fan can be obtained. Power module block and cooling system design flow chart are shown in Fig. 2(a) and Fig. 2(b) respectively.

The power relation is shown in Fig. 2(c), the thermal power P_m of power module block can be expressed as

$$P_m = P_p - P_c \tag{1}$$

where P_p is the input power from power losses of power devices and P_c is the cooling power of heatsink considered as output power.

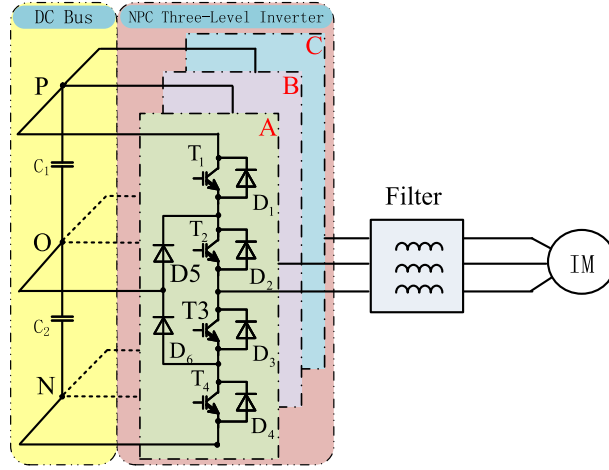
The power losses including switching loss and conducting loss will be calculated in this section. According to [19], the power losses of T_1, D_1, T_2, D_2 , and D_5 of upper bridge arm in phase A based on SVPWM modulation under unity power factor can be obtained as follows

$$P_{con, T_1}^{npc, svpwm} = \frac{mv_{0, T_1} I_m}{4\pi} ((\pi - \varphi) \cos \varphi + \frac{9}{8} \sin \varphi - \frac{1}{24} \sin 3\varphi) + \frac{mr_{T_1} I_m^2}{4\pi} \left(\frac{19}{18} + \frac{4}{3} \cos \varphi + \frac{7}{30} \cos 2\varphi - \frac{2}{45} \cos 3\varphi \right) \tag{2}$$

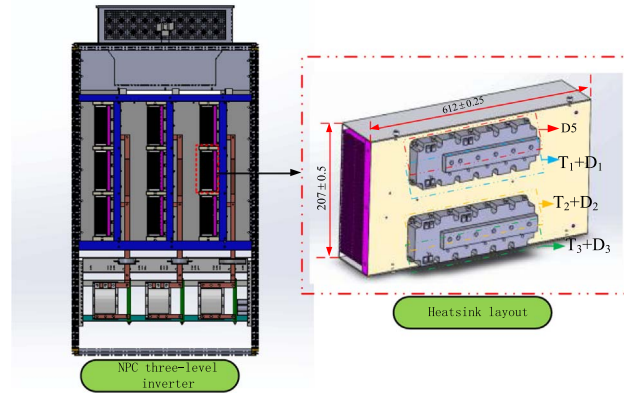
$$P_{sw, T_1}^{npc, svpwm} = \frac{f_{sw}}{2\pi} (A_{sw, T} I_m^2 \frac{1}{2} (\pi - \varphi + \frac{1}{2} \sin 2\varphi) + B_{sw, T} I_m (1 + \cos \varphi) + C_{sw, T} (\pi - \varphi)) \cdot \left(\frac{U_{dc}/2}{U_{base}} \right)^{D_{sw, T}} \left(\frac{T_{vj, T_1}}{T_{base}} \right)^{K_{sw, T}} \tag{3}$$

$$P_{con, D_1}^{npc, svpwm} = \frac{mv_{0, D_1} I_m}{4\pi} \left(\frac{9}{8} \sin \varphi - \varphi \cos \varphi - \frac{1}{24} \sin 3\varphi \right) + \frac{mr_{D_1} I_m^2}{4\pi} \left(\frac{19}{18} - \frac{4}{3} \cos \varphi + \frac{7}{30} \cos 2\varphi + \frac{2}{45} \cos 3\varphi \right) \tag{4}$$

$$P_{rec, D_1}^{npc, svpwm} = \frac{f_{sw}}{2\pi} (A_{rec, D} I_{pk}^2 \frac{1}{2} (\varphi - \frac{1}{2} \sin 2\varphi) + B_{rec, D} I_{pk} (1 - \cos \varphi) + C_{rec, D} \varphi) \cdot \left(\frac{U_{dc}/2}{U_{base}} \right)^{D_{rec, D}} \left(\frac{T_{vj, D_1}}{T_{base}} \right)^{K_{rec, D}} \tag{5}$$



(a) Topology of neutral point clamped three-level inverter.



(b) Structure and layout of inverter and heatsink

Fig. 1. Structure of inverter and cooling system. (a) Topology of neutral point clamped three-level inverter. (b) Structure and layout of inverter and heatsink.

$$P_{con,T_2}^{npc,svpwm} = \frac{v_{0,T_2} I_m}{\pi} + \frac{r_{T_2} I_m^2}{4} - \frac{mv_{0,T_2} I_m}{4\pi} \left(\frac{9}{8} \sin \varphi - \varphi \cos \varphi - \frac{1}{24} \sin 3\varphi \right) - \frac{mr_{T_2} I_m^2}{4\pi} \left(\frac{19}{18} - \frac{4}{3} \cos \varphi + \frac{7}{30} \cos 2\varphi + \frac{2}{45} \cos 3\varphi \right) \quad (6)$$

$$P_{sw,T_2}^{npc,svpwm} = \frac{f_{sw}}{2\pi} (A_{sw,T} I_m^2 \frac{1}{2} (\varphi - \frac{1}{2} \sin 2\varphi) + B_{sw,T} I_m (1 - \cos \varphi) + C_{sw,T} \varphi) \cdot \left(\frac{U_{dc}/2}{U_{base}} \right)^{D_{sw,T}} \left(\frac{T_{vj,T_2}}{T_{base}} \right)^{K_{sw,T}} \quad (7)$$

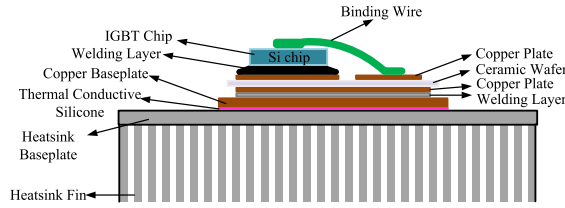
$$P_{con,D_2}^{npc,svpwm} = \frac{mv_{0,D_2} I_m}{4\pi} \left(\frac{9}{8} \sin \varphi - \varphi \cos \varphi - \frac{1}{24} \sin 3\varphi \right) + \frac{mr_{D_2} I_m^2}{4\pi} \left(\frac{19}{18} - \frac{4}{3} \cos \varphi + \frac{7}{30} \cos 2\varphi + \frac{2}{45} \cos 3\varphi \right) \quad (8)$$

$$P_{rec,D_2}^{npc,svpwm} = 0 \quad (9)$$

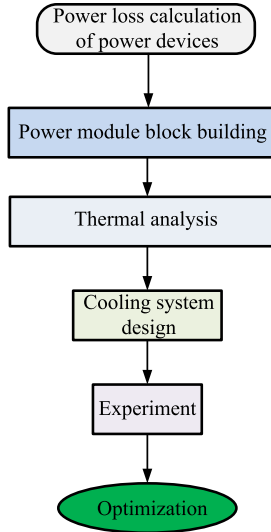
$$P_{con,D_5}^{npc,svpwm} = \frac{v_{0,D_5} I_m}{\pi} + \frac{r_{D_5} I_m^2}{4} - \frac{mv_{0,D_5} I_m}{2\pi} \left(\frac{19}{18} + \frac{7}{30} \cos 2\varphi \right) - \frac{mv_{0,D_5} I_m}{2\pi} \left(\frac{1}{2} \pi \cos \varphi - \varphi \cos \varphi + \frac{9}{8} \sin \varphi - \frac{1}{24} \sin 3\varphi \right) \quad (10)$$

$$P_{rec,D_5}^{npc,svpwm} = \frac{f_{sw}}{2\pi} (A_{rec,D} I_m^2 \frac{1}{2} (\pi - \varphi + \frac{1}{2} \sin 2\varphi) + B_{rec,D} I_m (1 + \cos \varphi) + C_{rec,D} (\pi - \varphi)) \cdot \left(\frac{U_{dc}/2}{U_{base}} \right)^{D_{rec,D}} \left(\frac{T_{vj,D_5}}{T_{base}} \right)^{K_{rec,D}} \quad (11)$$

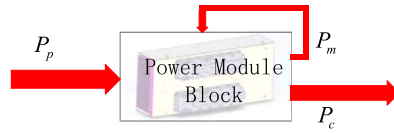
Therefore, power losses of T₁, D₁, T₂, D₂, and D₅ of upper bridge arm in phase A are



(a) Power module block.



(b) Flow chart of cooling system optimization strategy.



(c) Power relation

Fig. 2. Research objects (a) Power module block. (b) Flow chart of cooling system optimization strategy. (c) Power relation.

$$\begin{cases}
 P_{T_1}^{npc,svpwm} = P_{con,T_1}^{npc,svpwm} + P_{sw,T_1}^{npc,svpwm} \\
 P_{D_1}^{npc,svpwm} = P_{con,D_1}^{npc,svpwm} + P_{rec,D_1}^{npc,svpwm} \\
 P_{T_2}^{npc,svpwm} = P_{con,T_2}^{npc,svpwm} + P_{sw,T_2}^{npc,svpwm} \\
 P_{D_2}^{npc,svpwm} = P_{con,D_2}^{npc,svpwm} + P_{rec,D_2}^{npc,svpwm} \\
 P_{D_5}^{npc,svpwm} = P_{con,D_5}^{npc,svpwm} + P_{rec,D_5}^{npc,svpwm}
 \end{cases} \tag{12}$$

In (1)–(11), $D(\alpha) = m \sin \alpha$ expresses the modulation function; α stands for phase angle; φ stands for impedance angle; $D_{rec,D}$ is the correction coefficient to modify the testing voltage U_{base} ; $K_{rec,D}$ is the correction coefficient to modify testing junction temperature T_{base} ; $A_{rec,D}$, $B_{rec,D}$, and $C_{rec,D}$ are quadratic curve fitting coefficients of switching power loss under testing conditions, and they change with current dynamically; $v_{0,T_x} = v_{0,T}25^\circ C + K_{v0,T}(T_{vj,T_x} - 25^\circ C)$ expresses the xth IGBT's initial saturation voltage drop; $r_{T_x} = r_{T}25^\circ C + K_{r,T}(T_{vj,T_x} - 25^\circ C)$ expresses the xth IGBT's conducting resistance; $v_{0,D_x} = v_{0,D}25^\circ C + K_{v0,D}(T_{vj,D_x} - 25^\circ C)$ expresses the xth fast recovery diode's initial saturation voltage drop; $r_{D_x} = r_{D}25^\circ C + K_{r,D}(T_{vj,D_x} - 25^\circ C)$ expresses the fast recovery diode's conducting resistance; T_{vj,D_x} expresses the fast recovery diode's junction temperature; where $x=1,2$, and 5 ; $P_{con,T_1}^{npc,svpwm}$, $P_{con,D_1}^{npc,svpwm}$, $P_{con,T_2}^{npc,svpwm}$, $P_{con,D_2}^{npc,svpwm}$, $P_{con,D_5}^{npc,svpwm}$ stands for conducting power losses of T_1, D_1, T_2, D_2 , and D_5 respectively; $P_{sw,T_1}^{npc,svpwm}$ and $P_{sw,T_2}^{npc,svpwm}$ stands for switching power losses of T_1 and T_2 ; $P_{rec,D_1}^{npc,svpwm}$, $P_{rec,D_2}^{npc,svpwm}$, $P_{rec,D_5}^{npc,svpwm}$ stands for the reverse recovery power losses of D_1, D_2 , and D_5 [19].

Similarly, power losses of other power devices can be calculated including T_3 and D_3 .

Table 1
Parameters of induction motor.

Rated power P_d (kW)	475
Stator voltage U_s (V)	6000
Stator current I_d (A)	59
Rotor voltage U_r (V)	640
Rotor current I_r (A)	435
Rated speed (r/min)	735
Power factor	0.85

3. Cooling system design

The parameters of induction motor and inverter are shown in Tables 1 and 2 respectively.

Put these parameters into (1)–(11) to calculate power losses, and the results under rated conditions can be obtained and is shown in Fig. 6.

According to Fig. 3(a), the average power loss of D_1 is 35 W. In the same way, average power losses of D_2 , D_5 , T_1 , T_2 , and T_3 can be achieved and illustrated in Fig. 3(b).

The total power P_{total} of heatsink can be calculated from Fig. 3(b) and is shown as follow

$$P_{total} = 1890 \text{ W} = 1890 \text{ J/s} \tag{13}$$

The heatsink is fixed in this paper, which means the inverter structure immutable. The structure and parameter of heatsink are shown in Fig. 4(a) and (b). In this section, the cooling fan, acting as one of the most important devices in cooling system design, will be figured out. In accordance with thermal equilibrium equation, the cooling air flow can be expressed as

$$L = \frac{Q}{\rho C_p (t_o - t_i)} \tag{14}$$

where, L is the cooling air flow, m^3/s ; Q is the heat power from thermal source, kW; ρ is the air density, kg/m^3 ; C_p is the specific heat capacity of air, $\text{kJ}/(\text{kg}\cdot^\circ\text{C})$; t_o is the air temperature of wind outlet in heat-sink, $^\circ\text{C}$; t_i is the air temperature of wind inlet in heat-sink, $^\circ\text{C}$.

It is known from [20] that $\rho = 1.13 \text{ kg}/\text{m}^3$; $C_p = 1.005 \text{ kJ}/(\text{kg}\cdot^\circ\text{C})$; $t_o=55 \text{ }^\circ\text{C}$, which is the maximum permissible air temperature of heat-sink outlet; $t_i=30 \text{ }^\circ\text{C}$, which is the ambient temperature of heat-sink inlet. Put these parameters and $Q=P_{total}=1890 \text{ J/s}$ into (13), and cooling air flow will be solved as follow

$$L = \frac{Q}{\rho C_p (t_o - t_i)} = \frac{1890}{1.13 \times 1.005 \times (55 - 30)} = 239.7 \text{ m}^3/\text{h} \tag{15}$$

Take air leakage losses into consideration and improve the reliability of cooling system, L will be modified after repeated experiments as follow

$$L^* = \lambda \cdot L \tag{16}$$

where, L^* is the modified air flow value and λ is the modification factor, which is 1.2 in this paper. From (15), the modified air flow of single heat-sink is $287.6 \text{ m}^3/\text{h}$. But because of the existence of wind resistance, the air flow at operation point of cooling fan is typically less than maximum air volume. Therefore, it is necessary to figure out the operation point of the fan before completing the fan selection.

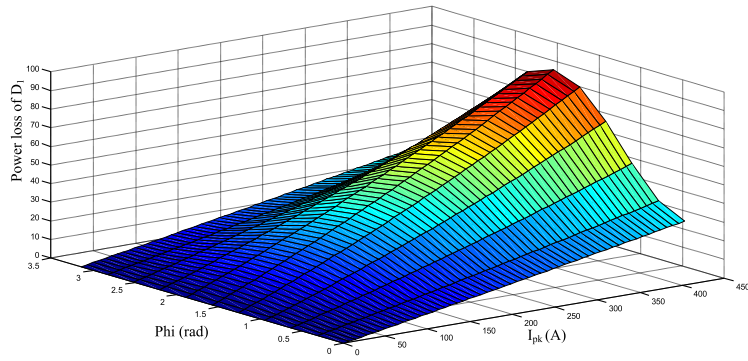
According to [20], when air flows in the channel, the friction pressure loss of unit channel length will be

$$R_m = \frac{\lambda}{4R_s} \cdot \frac{\nu^2}{2} \rho \tag{17}$$

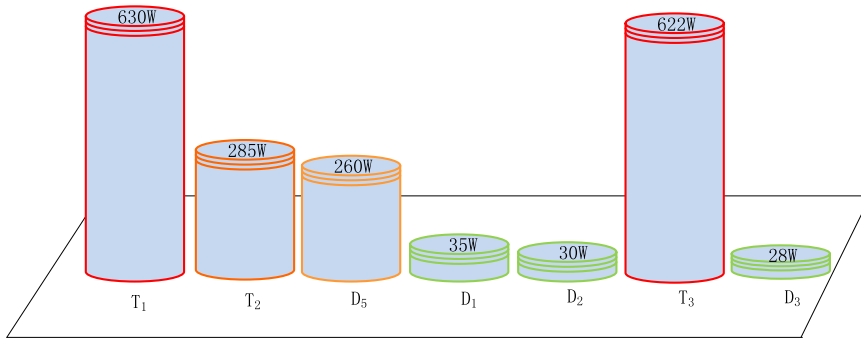
where, R_m is the friction pressure loss of unit length, Pa/m ; ν is the average velocity of air flowing in the duct, m/s ; ρ is the air density, kg/m^3 ; λ is the friction factor; R_s is the hydraulic radius of duct, m .

Table 2
Main parameters of inverter main circuit.

U_{dc}	1100 V
DC-link capacitor parameters	1800 $\mu\text{F}/1300 \text{ V}$
Power device parameters	Infineon, FF1400R17IE4 series
Switching frequency	2000 Hz



(a) Power Loss of D₁



(b) Power losses of all devices on heat-sink module block

Fig. 3. Power losses of power devices (a) Power loss of D₁. (b) Power losses of all devices on heat-sink module block.

$$R_s = \frac{ab}{2(a + b)} \tag{18}$$

where a and b are the lengths of rectangular duct, m.

The heatsink length y is also the duct length, and the duct resistance is

$$R_m = \frac{\lambda}{4R_s} \cdot \frac{L^2}{2} \rho y \tag{19}$$

In this paper, $a = 2.5$ mm , $b = 8.3$ mm , $y = 612$ mm , and average roughness of air duct $\epsilon = 25$ μ m. Put these parameters into (17), and R_s can be calculated as follow

$$R_s = 0.96 \text{ mm} \tag{20}$$

Equivalent diameter of duct can be obtained as well from the following equation

$$d = \frac{2ab}{(a + b)} = 3.84 \text{ mm} \tag{21}$$

The relative roughness of duct can be calculated as follow

$$\epsilon/d = 6.5 \times 10^{-3} \tag{22}$$

Through checking the relative roughness and friction coefficient table [20], it is known that $\lambda = 0.032$.

The relationship between air velocity v_c and air volume L_c is

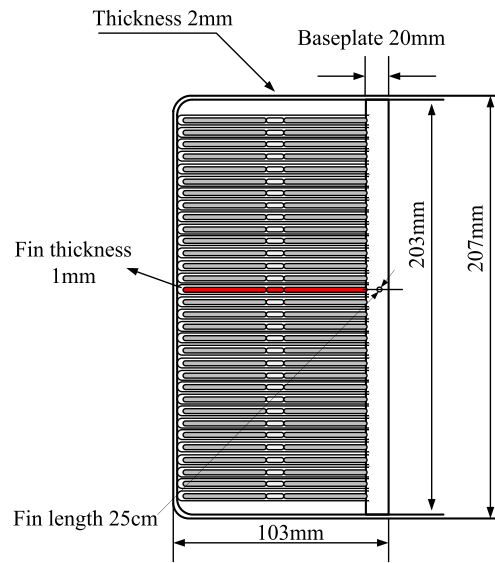
$$v_c = L_c / (y \cdot n \cdot a \cdot b) = 0.515 L_c \tag{23}$$

where, n is the fin number, $n=26$. At this time the unit of air volume is m^3/min .

Put (21) and (22) into (18), and R_m can be expressed as follow

$$R_m = 2.8815 v^2 = 0.75 L_c^2 \tag{24}$$

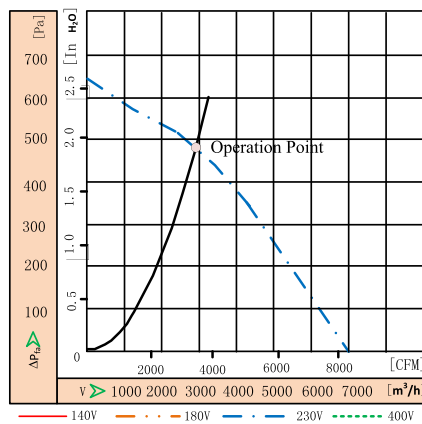
The relationship between air volume and air resistance can be found in (23) and the characteristic curve of fan is shown in



(a) Structure and parameter of heatsink



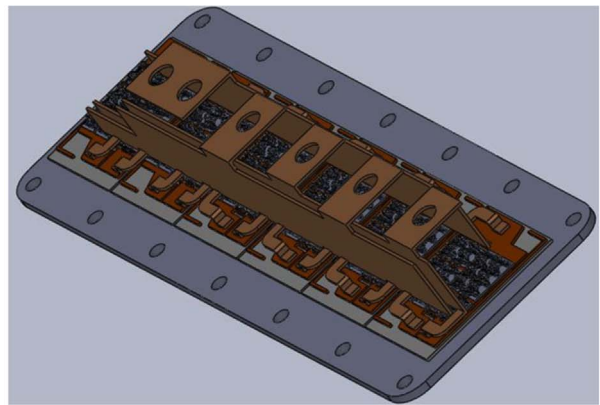
(b) Material object of power module block



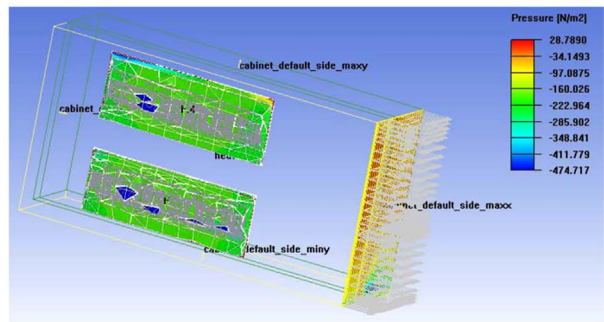
(c) Characteristic curve of cooling fan

Fig. 4. Cooling system design

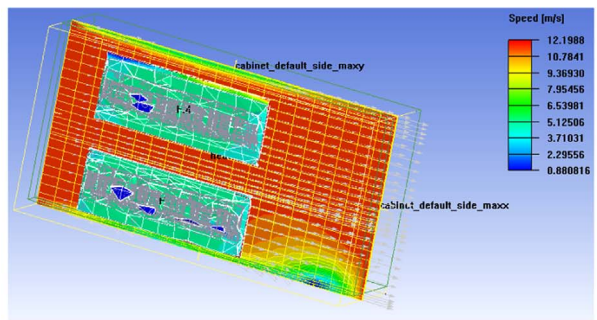
Fig. 4. Cooling system design (a) Structure and parameter of heatsink (b) Material object of power module block. (c) Characteristic curve of cooling fan.



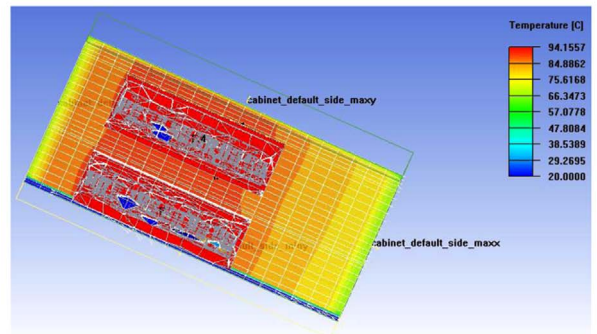
(a) IGBT solid model



(b) Pressure simulation of heatsink outlet



(c) Air velocity simulation of heatsink

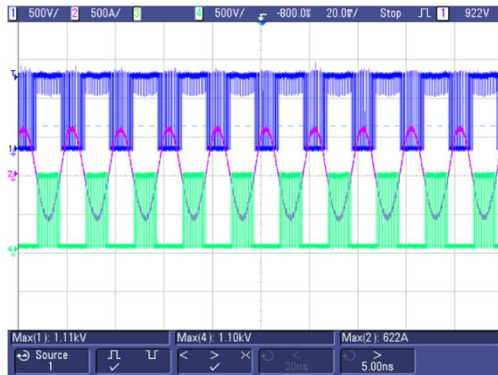


(d) Temperature simulation of power module block

Fig. 5. Modeling and simulation, (a) IGBT solid model. (b) Pressure simulation of heatsink outlet. (c) Air velocity simulation of heatsink. (d) Temperature simulation of power module block.



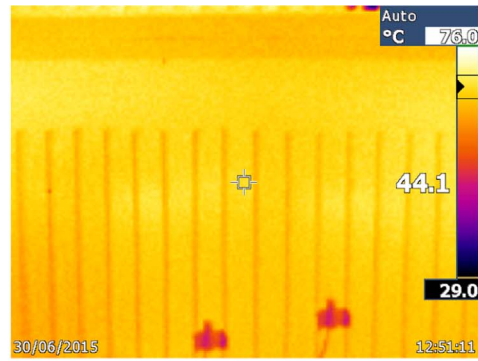
(a) Experiment platform



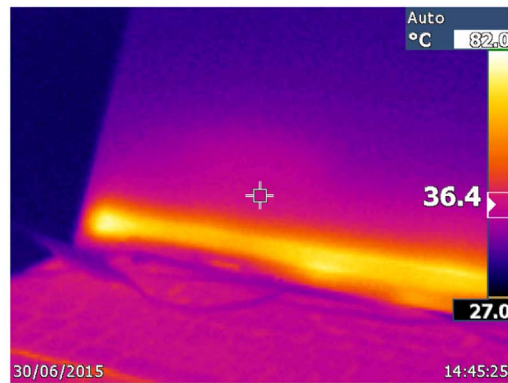
(b) Waveforms of T_1 and output current



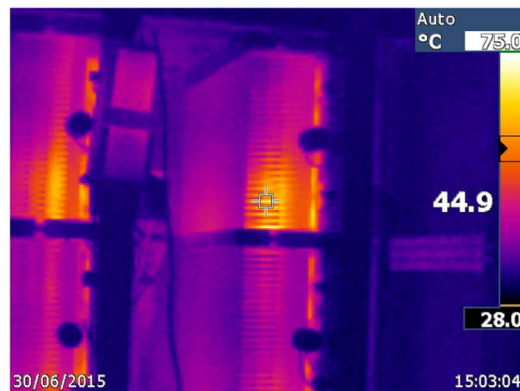
(c) Air velocity



(d) Basedplate temperature of heatsink



(e) Baseplate temperature of IGBT module



(f) Temperature of power module block

Fig. 6. Experiment platform and results. (a) Experiment platform. (b) Waveforms of T_1 and output current. (c) Air velocity (d) Basedplate temperature of heatsink. (e) Baseplate temperature of IGBT module. (f) Temperature of power module block.

Fig. 4(c).

4. Simulation and experiment

The solid model of IGBT inner module is shown in Fig. 5(a). The simulation parameters of the NPC three-level inverter were shown in Tables 1 and 2. What's more, the simulation of the inverter system was finished after the appearance of the thermal stability of forced-air cooling system.

The material object of power module block is shown in Fig. 4(a). The simulation parameters of forced-air cooling system come from the cooling system design in Section III, and the simulation was conducted until the thermal stability of the inverter system. In this simulation and experiment the thermal stability was realized at the 45th minute after the beginning.

It can be seen by analyzing Fig. 5(a)–(d) that the maximum static pressure of heat-sink is 474 Pa, the average air velocity is 11 m/s approximately, and the maximum junction temperature of power devices is 94 °C approximately. What's more, it can be observed from Fig. 5(d) that the baseplate temperature of IGBT module is lower than junction temperature by 10 °C and the temperature of heat-sink baseplate, which contacts with IGBT module directly, is lower than junction temperature by 20 °C. But the temperature of whole power module block is under 125 °C and is within the temperature range of safe working.

Experiment platform and results are shown in Fig. 6, and the following results are captured after the whole system running into steady state under rated conditions.

The experiment platform is shown in Fig. 6(a). It can be seen from Fig. 6(b) that NPC three-level inverter based on SVPWM modulation has a good electrical performance. In Fig. 6(c), the air velocity is 10.51 m/s, 0.5 m/s smaller than simulation value approximately. From Fig. 6(d) and (e), it can be found that the maximum temperatures of heat-sink basedplate and IGBT module baseplate are 76 °C and 82 °C respectively, with a 6 °C temperature difference. Finally, it can be observed from Fig. 6(f) that the maximum temperature of power module block under steady state is 75 °C. It must be pointed out that the IGBT module baseplate captured in Fig. 6(f) is the upper part which is exposed to the air and has a lower temperature. Above all, the experiment results are consistent with the results of former analysis, and the junction temperature can be estimated at 102 °C approximately, lower than the maximum allowable temperature of power devices. The experiment proved the feasibility of the proposed method that analyzing single power module block can provide reference during cooling system design, which can connect power losses of power losses with the forced-air cooling system design to complete the aided design of the high-power NPC three-level inverter system.

5. Conclusions

A method based on analysis of single power module block for cooling system design of NPC three-level inverter was put forward. It has completed power loss calculation of power module block, theory calculation of heat-sink parameter, characteristic parameters calculation of cooling fan, and finally cooling fan selection. The power loss calculation of power devices and thermal model building of power module block were finished separately, but the analysis was made under the combination of the two modules to avoid these ideal assumptions in traditional algorithms, such as absolute smooth in contact surface and absolute excellent contact. The method proposed in this paper has a much higher accuracy compared with the traditional ones. Through finite element simulation, the power module block was analyzed. The effectiveness and feasibility of the proposed method was proved by experiment.

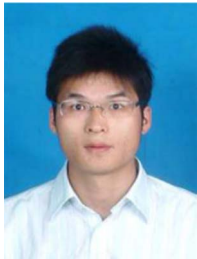
Acknowledgement

The authors would like to thank Science and Technology Program of Henan, Grant No. 162102210266 and Doctoral Scientific Research Start-up Foundation of Henan Normal University, Grant No. 5101029170276.

References

- [1] Wang Qunjing, Chen Quan, Jiang Weidong, Hu Cungang, Analysis of conduction losses in neutral-point-clamped three-level inverter, *Trans. China Electrotech. Soc.* 22 (3) (2007) 66–70.
- [2] T.J. Kim, D.W. Kang, Y.H. Lee, D.S. Hyun, The analysis of conduction and switching losses in multi-level inverter system, *PESC Rec. - IEEE Annu. Power Electron. Spec. Conf.* 3 (2001) 1363–1368 (vol. 3).
- [3] Wei Jing, Study on Power Device Losses of High-Power Three-Level Converter[D].XUZHOU, China University of Mining and Technology, 2010 http://epub.cnki.net/kns/brief/default_result.aspx.
- [4] J. Bednarčík, E. Burkel, K. Saksl, P. Kollár, S. Roth, Comparison of losses and thermal performance of a three-level three-phase neutral-point-clamped dc-ac converter under a conventional NTV and the NTV2 modulation strategies, in: *Proceedings of the 32nd Annual Conference on IEEE Industrial Electronics IECON*, vol.100, 2006, pp. 4819–4824.
- [5] S.S. Fazel, D. Krug, T. Taleb, S. Bernet, Comparison of power semiconductor utilization, losses and harmonic spectra of state-of-the-art 4.16kV multi-level voltage source converters, in: *Proceedings of the European Conference on Power Electronics and Applications, IEEE*, 2005 (pp.11 pp.-P.11).
- [6] C.S. Yun, P. Malberti, M. Ciappa, W. Fichtner, Thermal component model for electrothermal analysis of igbt module systems, *IEEE Trans. Adv. Packag.* 24 (3) (2001) 401–406.
- [7] D.U. Yi, M.Y. Liao, Losses calculation of igbt module and heat dissipation system design of inverters, *Electr. Drive Autom.* 24 (3) (2011) 159–163.
- [8] Quan Chen, Wang Qunjing, Jiang Weidong, Hu Cungang, Analysis of switching losses in diode-clamped three-level converter, *Trans. China Electrotech. Soc.* (2008).
- [9] I. Swan, A. Bryant, P.A. Mawby, T. Ueta, T. Nishijima, K. Hamada, A fast loss and temperature simulation method for power converters, part ii: 3-d thermal model of power module, *IEEE Trans. Power Electron.* 27 (1) (2012) 258–268.
- [10] J. Liu, L. Huang, Thermal analysis of igbt module based on the software of ansys, *Power Electron.* (2013).
- [11] U. Drogenik, G. Laimer, J.W. Kolar, Theoretical converter power density limits for forced convection cooling, in: *Proceedings of the International PCIM Europe*

- 2005 Conference, 2005, pp. 608–619
- [12] U. Drogenik, J.W. Kolar, Analyzing the theoretical limits of forced air-cooling by employing advanced composite materials with thermal conductivities > 400 W/mK. in: Proceedings of the 4th International Conference on Integrated Power Systems (CIPS) VDE, 2006, pp. 1–6.
- [13] (J) E.M. Sparrow, B.R. Baliga, S.V. Patankar, Forced convection heat transfer from a shrouded fin array with and without tip clearance. *J. Heat. Transf.* 100 (4) (1978) 572–579.
- [14] W. Leonard, P. Teertstra, J.R. Culham, A. Zagher, Characterization of Heat Sink Flow Bypass in Plate Fin Heat Sinks. *ASME 2002 International Mechanical Engineering Congress and Exposition, American Society of Mechanical Engineers, 2002*, pp. 189–196.
- [15] P. Ning, F. Wang, K.D. Ngo, Forced-air cooling system design under weight constraint for high-temperature SiC converter, *IEEE Trans. Power Electron.* 29 (4) (2014) 1998–2007.
- [16] M.M. Ayadi, M.A. Fakhfakh, M. Ghariani, R. Neji, M.M. Ayadi, M. Ghariani, Electro-thermal simulation of a three phase inverter with cooling system, *J. Model. Simul. Syst.* (3) (2010).
- [17] A. Lakhsasi, Y. Hamri, A. Skorek, Partially coupled electro-thermal analysis for accurate prediction of switching devices, *Can. Conf. Electr. Comput. Eng.* 1 (2001) 375–380.
- [18] M. Honsberg, T. Radke, 3-level IGBT modules with trench gate IGBT and their thermal analysis in UPS, PFC and PV operation modes, in: Proceedings of the 13th European Conference on Power Electronics and Applications, EPE '09., IEEE, 2009, pp. 1 – 7.
- [19] Wei Jing, Study on power device losses of high-power three-level Converter[D]. XUZHOU, China Univ. Min. Technol. (2010).
- [20] Zhong-hai zhang, The electronic devices of high power devices forced air cooling heat system design, *Electron. Mech. Eng.* 21 (3) (2005) 18–21.



Shi-Zhou Xu was born in Henan province, China, in 1985. He received the M.S. and Ph.D. degree of electrical engineering from China University of Mining and Technology (Xuzhou, China) respectively in 2009 and 2012. His current research interests include cooling system thermal optimization, laminated busbar research, and high-power three-level inverter modeling, control and improvement.